NIH Public Access
Author Manuscript
Nature. Author manuscript; available in PMC 2014 August 09.

Published in final edited form as:
Nature. 2014 February 6; 506(7486): 97–101. doi:10.1038/nature12828.

Sequence variants in *SLC16A11* are a common risk factor for type 2 diabetes in Mexico

The SIGMA (Slim Initiative in Genomic Medicine for the Americas) Type 2 Diabetes Consortium

Abstract

Performing genetic studies in multiple human populations can identify disease risk alleles that are common in one population but rare in others[1], with the potential to illuminate pathophysiology, health disparities, and the population genetic origins of disease alleles. We analyzed 9.2 million single nucleotide polymorphisms (SNPs) in each of 8,214 Mexicans and Latin Americans: 3,848 with type 2 diabetes (T2D) and 4,366 non-diabetic controls. In addition to replicating previous findings[2–4], we identified a novel locus associated with T2D at genome-wide significance spanning the solute carriers *SLC16A11* and *SLC16A13* (P=3.9×10^{-13}; odds ratio (OR)=1.29). The association was stronger in younger, leaner people with T2D, and replicated in independent samples (P=1.1×10^{-4}; OR=1.20). The risk haplotype carries four amino acid substitutions, all in SLC16A11; it is present at ≈50% frequency in Native American samples and ≈10% in East Asian, but rare in European and African samples. Analysis of an archaic genome sequence indicated the risk haplotype introgressed into modern humans via admixture with Neandertals. The *SLC16A11* mRNA is expressed in liver, and V5-tagged SLC16A11 protein localizes to the endoplasmic reticulum. Expression of SLC16A11 in heterologous cells alters lipid metabolism, most notably causing an increase in intracellular triacylglycerol levels. Despite T2D having been well studied by genome-wide association studies (GWAS) in other populations, analysis in Mexican and Latin American individuals identified *SLC16A11* as a novel candidate gene for T2D with a possible role in triacylglycerol metabolism.

The Slim Initiative in Genomic Medicine for the Americas (SIGMA) Type 2 Diabetes Consortium set out to characterize the genetic basis of T2D in Mexican and Latin American populations, where the prevalence is roughly twice that of U.S. non-Hispanic whites[5,6]. This report considers 3,848 T2D cases and 4,366 controls (Table 1) genotyped using the Illumina OMNI 2.5 array that were unrelated to other samples, and that fall on a cline of Native American and European ancestry[7] (Extended Data Fig. 1). Association analysis included 9.2 million variants that were imputed[8,9] from the 1,000 Genomes Project Phase I release[10] based on 1.38 million SNPs directly genotyped at high quality with minor allele frequency (MAF) >1%.

The association of SNP genotype with T2D was evaluated using LTSOFT[11], a method that increases power by jointly modeling case-control status with non-genetic risk factors. Our analysis utilized body mass index (BMI) and age to construct liability scores and also

---

The authors declare no competing financial interests.

NIH-PA Author Manuscript
NIH-PA Author Manuscript
NIH-PA Author Manuscript

NIH-PA Author Manuscript
NIH-PA Author Manuscript
NIH-PA Author Manuscript

included adjustment for sex and ancestry via principal components[7]. The quantile-quantile (QQ) plot is well calibrated under the null (λ_{GC} = 1.05; Fig. 1a, *red*), indicating adequate control for confounders, with substantial excess signal at $P<10^{-4}$.

We first examined SNPs previously reported to be associated to risk of T2D. Two such variants reached genome-wide significance: *TCF7L2* (rs7903146; $P=2.5\times10^{-17}$; OR=1.41 [95% confidence interval 1.30–1.53]) and *KCNQ1* (rs2237897; $P=4.9\times10^{-16}$; OR=0.74 [0.69–0.80]) (Extended Data Figs. 2, 3a), with effect sizes and frequencies consistent with previous studies[3,4,12]. At *KCNQ1*, we identified a signal[3] of association that shows limited linkage disequilibrium both to rs2237897 (r^2=0.056) and to rs231362 (r^2=0.028) (previously seen in Europeans), suggesting a third allele at this locus (rs139647931; after conditioning, $P=5.3\times10^{-8}$; OR=0.78 [0.70–0.86]; Extended Data Fig. 3b; Supplementary Note).

More generally, of SNPs previously associated with T2D at genome-wide significance, 56 of 68 are directionally consistent with the initial report ($P=3.1\times10^{-8}$; Supplementary Table 1). Nonetheless, a QQ plot excluding all SNPs within 1 Mb of the 68 T2D associations remains strikingly non-null (Fig. 1a, *blue*).

This excess signal of association is entirely attributable to two regions of the genome: chromosome 11p15.5 and 17p13.1 (Fig. 1a, *black*). The genome-wide significant association at 11p15.5 spans insulin, *IGF2*, and other genes (Extended Data Fig. 3a). The strongest association lies in the 3′-UTR of *IGF2* and the non-coding *INS-IGF2* transcript (rs11564732, $P=2.6\times10^{-8}$; OR=0.77 [0.70–0.84]; Supplementary Table 2). The associated SNPs are ~700 kb from the genome-wide significant signal in *KCNQ1* (above), and analysis conditional on the two significant *KCNQ1* SNPs reduced the *INS-IGF2* association signal to just below genome-wide significance ($P=7.5\times10^{-7}$, Extended Data Fig. 3c). Conditioning on the two *KCNQ1* SNPs and the *INS-IGF2* SNP reduces the signal to background (Extended Data Fig. 3d). Further analysis is needed to determine whether the *INS-IGF2* signal is reproducible and independent of that at *KCNQ1*.

The strongest novel association is at 17p13.1 spanning *SLC16A11* and *SLC16A13* (Fig. 1b), both poorly characterized members of the monocarboxylic acid transporter family of solute carriers[13]. The strongest signal of association includes a silent mutation as well as four missense SNPs, all in SLC16A11 (Fig. 1d, e). These five variants are (a) in strong LD ($r^2 \geq$ 0.85 in 1,000 Genomes samples from the Americas) and co-segregate on a single haplotype, (b) common in samples of Mexican and Latin American ancestry, and (c) show equivalent levels of association to T2D ($P=2.4\times10^{-12}$ to $P=3.9\times10^{-13}$; OR=1.29 [1.20–1.38]; Supplementary Tables 3, 4, and 5). Analysis conditional on any of these variants leaves no genome-wide significant signal (Fig. 1c, Extended Data Fig. 4). Computational prediction with SIFT[14] (which considers each site independently) labels one of the missense SNPs (rs13342692, D127G) as damaging and the other three “tolerated” (Supplementary Table 6).

Individuals with T2D that carry the risk haplotype develop T2D 2.1 years earlier ($P=3.1\times10^{-4}$), and at 0.9 kg/m^2 lower BMI ($P=5.2\times10^{-4}$) than non-carriers (Extended Data Fig. 5). The odds ratio for the risk haplotype estimated using young cases (≤ 45 years) was higher than in older cases (OR=1.48 versus 1.11; $P_{heterogeneity}=1.7\times10^{-3}$). We tested the

NIH-PA Author Manuscript
NIH-PA Author Manuscript
NIH-PA Author Manuscript

haplotype for association with related metabolic quantitative traits in the fasting state in a subset of SIGMA participants (n=1,505–3,855). No associations surpass nominal significance (P<0.05; Supplementary Table 7).

Given that large GWAS have been performed for T2D in samples of European and Asian ancestry, it may seem surprising that associated variants at *SLC16A11/13* were not previously identified. Using data generated by the 1,000 Genomes Project and the current study, we observed that the risk haplotype (henceforth referred to as "5 SNP" haplotype) is rare or absent in samples from Europe and Africa, has intermediate frequency (≈10%) in samples from East Asia, and up to ≈50% frequency in samples from the Americas (Fig. 1d; Extended Data Fig. 6a). A second haplotype carrying one of the four missense SNPs (D127G) and the synonymous variant (termed the "2 SNP" haplotype) is very common in samples from Africa but rare elsewhere, including in the Americas (Fig. 1d). The low frequency of the 5 SNP haplotype in Africa and Europe may explain why this association was not found in previous studies.

We attempted to replicate this association in ~22,000 samples from a variety of ancestry groups. A proxy for the 5 SNP haplotype of *SLC16A11* showed strong association with T2D ($P_{replicaton}=1.1\times10^{-4}$; $OR_{replication}=1.20$ [1.09–1.31]; $P_{combined}=5.4\times10^{-15}$; $OR_{combined}=1.25$ [1.18–1.32]; Fig. 1f; Supplementary Table 8). The association was clearly observed in East Asian samples, a population which lacks admixture of Amerindian and European populations and shows little genetic substructure. This result argues against population stratification as an explanation for the finding in Latino populations.

We estimated the difference in disease prevalence attributable to a risk factor with OR=1.20 (1.09–1.31), 26% frequency in Mexican Americans (as in the SIGMA control samples), and 2% in European Americans. Approximately 20% (9.2%-29%) of the difference in prevalence could be explained by such a risk factor (Online Methods).

Two population genetic features of the 5 SNP haplotype struck us as discordant. The haplotype sequence is highly divergent, with an estimated time to most recent common ancestor (TMRCA) of 799k years to a European haplotype (Supplementary Table 9 and Supplementary Note). This long precedes the "out of Africa" bottleneck. And yet, the haplotype is not observed in Africa and is rare throughout Europe (Fig. 1d).

This combination of age and geographic distribution could be consistent with admixture from Neandertals into modern humans. Neither the published Neandertal genome[15] nor the Denisova genome[16] contained the variants observed on the 5 SNP haplotype. However, an unpublished genome of a Neandertal from Denisova Cave[17,18] is homozygous across 5 kb for the 5 SNP haplotype at *SLC16A11*, including all four missense SNPs. Over a span of 73 kb this Neandertal sequence is nearly identical to that of individuals from the 1000 Genomes Project who are homozygous for the 5 SNP haplotype (Supplementary Note).

Two lines of evidence suggest that the 5 SNP haplotype entered modern humans through archaic admixture. First, the Neandertal sequence is more closely related to the 5 SNP haplotype than to random non-risk haplotypes (mean TMRCA=250k years versus 677k years; Supplementary Tables 10 and 11, Supplementary Note), forming a clade (Extended

NIH-PA Author Manuscript

NIH-PA Author Manuscript

NIH-PA Author Manuscript

Data Fig. 6b), with a coalescence time that postdates the range of estimated split times between modern humans and Neandertals[16,19]. Second, the genetic length of the 73 kb haplotype is longer than would be expected if it had undergone recombination for ~9,000 generations since the split with Neandertals (P=3.9×10^{-5}; Supplementary Note). These two features indicate that the 5 SNP haplotype is not only similar to the Neandertal sequence, but was likely introduced into modern humans relatively recently through archaic admixture. We note that while this particular Neandertal-derived haplotype is common in the Americas, Latin Americans have the same proportion of Neandertal ancestry genome-wide as other Eurasian populations (~2%)[16].

With an absence of multiple independently segregating functional mutations in the same gene, we lack formal genetic proof that *SLC16A11* is the gene responsible for association to T2D at 17p13.1. Nonetheless, as the associated haplotype encodes four missense SNPs in a single gene (Supplementary Table 12), we set out to begin characterizing the function of SLC16A11.

We examined the tissue distribution of *SLC16A11* mRNA expression using Nanostring and ~55,000 curated microarray samples. In both datasets, we observed *SLC16A11* expression in liver, salivary gland, and thyroid (Extended Data Figs. 7 and 8). We used immunofluorescence to determine the subcellular localization of V5-tagged SLC16A11 introduced into HeLa cells. SLC16A11-V5 co-localizes with the endoplasmic reticulum membrane protein Calnexin, but shows minimal overlap with plasma membrane, Golgi apparatus and mitochondria (Fig. 2a). Distinct patterns were seen for other SLC16 family members, which are known to have diverse cellular functions[20]: SLC16A13-V5 localizes to the Golgi apparatus and SLC16A1-V5 appears at the plasma membrane[21] (Extended Data Fig. 9, data not shown).

As SLC16 family members are solute carriers, we expressed SLC16A11 (or control proteins) in HeLa cells (which do not express SLC16A11 at appreciable levels) and profiled ~300 polar and lipid metabolites. Expression of SLC16A11 resulted in substantial increases in triacylglycerol (TAG) levels (P=7.6×10^{-12}), with smaller increases in intracellular diacylglycerols (P=7.8×10^{-3}) and decreases in lysophosphatidylcholine (P=2.0×10^{-3}), cholesterol ester (P=9.8×10^{-4}) and sphingomyelin (P=3.9×10^{-3}) lipids (Fig. 2b, c, Supplementary Tables 13 and 14). As TAG synthesis takes place in the endoplasmic reticulum in the liver[22], these results suggest that SLC16A11 may play a role in hepatic lipid metabolism. We note that serum levels of specific TAGs have been prospectively associated with future risk of T2D[23] and accumulation of intracellular lipids has been implicated in insulin resistance in human populations[24,25].

In summary, GWAS in Mexican and Latin American samples identified a haplotype containing four missense SNPs, all in *SLC16A11*, that is much more common in individuals with Native American ancestry than in other populations. Each haplotype copy is associated with a ~20% increased risk of T2D. With these properties, the haplotype would be expected to contribute to the higher burden of T2D in Mexican and Latin American populations[26]. The haplotype derives from Neandertal introgression, providing an example of Neandertal admixture affecting physiology and disease susceptibility today. Our data suggest the

NIH-PA Author Manuscript

NIH-PA Author Manuscript

NIH-PA Author Manuscript

hypothesis for future studies that *SLC16A11* may influence diabetes risk through effects on lipid metabolism in the liver. Our results also indicate that genetic mapping in understudied populations can identify previously undiscovered aspects of disease pathophysiology[1].

Methods Summary

DNA samples were prepared using strict quality control procedures and genotyped using the Illumina HumanOmni2.5 array. Stringent sample and SNP quality (including ancestry) filters were applied on the resulting genotypes. Following imputation[8,9], SNPs were quality filtered (MAF ≥ 1% and info score ≥ .6) and association testing was performed via LTSOFT[11] with T2D status, BMI, and age modeling liability and adjusting for sex and top 2 principal components as fixed effect covariates. P-values were corrected for genomic control (λ_{GC}=1.046). Odds ratios (ORs) are from logistic regression in PLINK[27] using BMI, age, sex, and top 2 PCs as covariates. Proportion of Native American ancestry was estimated using ADMIXTURE[28] (*K*=3) run including unadmixed individuals from several populations.

Odds ratios for young (≤45 years) and older age of onset cases were calculated using logistic regression in each group compared to two randomly selected non-overlapping sets of controls. Significance testing used a Z-score calculated from these ORs.

Population prevalence was modeled using OR to approximate relative risk in a log-additive effect model[29]. Relative change in population prevalences is reported based on removing a locus with relative risk of 1.20 and the indicated frequency.

Gene expression analyses were performed on data collected using Nanostring and a compendium of publicly available Affymetrix U133 Plus 2.0 microarrays. The subcellular localization of SLC16A11-V5 and metabolic profiling studies were performed following expression of C-terminus, V5-tagged SLC16A11 in HeLa cells. Metabolite values were normalized to the total metabolite signal obtained for each sample. Measurements were obtained in replicate from each of three independent experiments, with data combined after subtracting the mean of the log-transformed values. The Wilcox rank sum test was used to test for differences in individual metabolite levels in cells expressing SLC16A11 compared to controls; the Wilcoxon signed rank test was used to assess differences in lipid classes.

Supplementary Material

Refer to Web version on PubMed Central for supplementary material.

Acknowledgments

We thank Mark Daly, Vamsi Mootha, Eric Lander and Karol Estrada for comments on the manuscript, Benjamin Voight, Ayellet Segre, Joseph Pickrell and the Scientific Advisory Board of the SIGMA Project (especially Carlos Bustamante) for useful discussions, and Aravind Subramanian and Victor Rusu for assistance with expression analyses. This work was conducted as part of the Slim Initiative for Genomic Medicine, a joint U.S.-Mexico project funded by the Carlos Slim Health Institute. The UNAM/INCMNSZ diabetes study was supported by Consejo Nacional de Ciencia y Tecnología grants 138826, 128877, CONACyT- SALUD 2009-01-115250, and a grant from Dirección General de Asuntos del Personal Académico, UNAM, IT 214711. The Diabetes in Mexico Study was supported by Consejo Nacional de Ciencia y Tecnología grant 86867 and by Instituto Carlos Slim de la Salud, A.C. The Mexico City Diabetes Study was supported by National Institutes of Health (NIH) grant R01HL24799 and by

NIH-PA Author Manuscript

NIH-PA Author Manuscript

NIH-PA Author Manuscript

the Consejo Nacional de Ciencia y Tenologia grants: 2092, M9303, F677-M9407, 251M, and 2005-C01-14502, SALUD 2010-2-151165. The Multiethnic Cohort was supported by NIH grants CA164973, CA054281, and CA063464. The Singapore Chinese Health Study was funded by the National Medical Research Council of Singapore under its individual research grant scheme and by NIH grants R01 CA55069, R35 CA53890, R01 CA80205, and R01 CA144034. The Type 2 Diabetes Genetic Exploration by Next-generation sequencing in multi-Ethnic Samples (T2D-GENES) project was supported by NIH grant U01DK085526. The San Antonio Mexican American Family Studies (SAMAFS) were supported by R01 DK042273, R01 DK047482, R01 DK053889, R01 DK057295, P01 HL045522, and a Veterans Administration Epidemiologic grant to R.A.D. A.L.W. is supported by National Institutes of Health Ruth L. Kirschstein National Research Service Award number F32 HG005944.

References

1. Rosenberg NA, et al. Genome-wide association studies in diverse populations. Nature reviews. Genetics. 2010; 11:356–366.
2. Grant SFA, et al. Variant of transcription factor 7-like 2 (TCF7L2) gene confers risk of type 2 diabetes. Nature genetics. 2006; 38:320–323. doi:http://www.nature.com/ng/journal/v38/n3/suppinfo/ng1732_S1.html. [PubMed: 16415884]
3. Unoki H, et al. SNPs in KCNQ1 are associated with susceptibility to type 2 diabetes in East Asian and European populations. Nature genetics. 2008; 40:1098–1102. doi:http://www.nature.com/ng/journal/v40/n9/suppinfo/ng.208_S1.html. [PubMed: 18711366]
4. Yasuda K, et al. Variants in KCNQ1 are associated with susceptibility to type 2 diabetes mellitus. Nature genetics. 2008; 40:1092–1097. doi:http://www.nature.com/ng/journal/v40/n9/suppinfo/ng.207_S1.html. [PubMed: 18711367]
5. Villalpando S, et al. Prevalence and distribution of type 2 diabetes mellitus in Mexican adult population: a probabilistic survey. Salud Pública de México. 2010; 52:S19–S26. [PubMed: 20585724]
6. U.S. Department of Health and Human Services, Centers for Disease Control and Prevention; Atlanta, GA: 2011.
7. Patterson N, Price AL, Reich D. Population Structure and Eigenanalysis. PLoS genetics. 2006; 2:e190.10.1371/journal.pgen.0020190 [PubMed: 17194218]
8. Howie BN, Donnelly P, Marchini J. A Flexible and Accurate Genotype Imputation Method for the Next Generation of Genome-Wide Association Studies. PLoS genetics. 2009; 5:e1000529.10.1371/journal.pgen.1000529 [PubMed: 19543373]
9. Williams, Amy L.; Patterson, N.; Glessner, J.; Hakonarson, H.; Reich, D. Phasing of Many Thousands of Genotyped Samples. American journal of human genetics. 2012; 91:238–251. [PubMed: 22883141]
10. An integrated map of genetic variation from 1,092 human genomes. Nature. 2012; 491:56–65. doi:http://www.nature.com/nature/journal/v491/n7422/abs/nature11632.html#supplementary-information. [PubMed: 23128226]
11. Zaitlen N, et al. Informed Conditioning on Clinical Covariates Increases Power in Case-Control Association Studies. PLoS genetics. 2012; 8:e1003032.10.1371/journal.pgen.1003032 [PubMed: 23144628]
12. Voight BF, et al. Twelve type 2 diabetes susceptibility loci identified through large-scale association analysis. Nature genetics. 2010; 42:579–589. doi:http://www.nature.com/ng/journal/v42/n7/suppinfo/ng.609_S1.html. [PubMed: 20581827]
13. Halestrap AP. The monocarboxylate transporter family—Structure and functional characterization. IUBMB Life. 2012; 64:1–9.10.1002/iub.573 [PubMed: 22131303]
14. Ng PC, Henikoff S. SIFT: predicting amino acid changes that affect protein function. Nucleic acids research. 2003; 31:3812–3814.10.1093/nar/gkg509 [PubMed: 12824425]
15. Green RE, et al. A Draft Sequence of the Neandertal Genome. Science. 2010; 328:710–722.10.1126/science.1188021 [PubMed: 20448178]
16. Meyer M, et al. A High-Coverage Genome Sequence from an Archaic Denisovan Individual. Science. 201210.1126/science.1224344

NIH-PA Author Manuscript
NIH-PA Author Manuscript
NIH-PA Author Manuscript

17. Mednikova MB. A proximal pedal phalanx of a Paleolithic hominin from denisova cave, Altai. Archaeology, Ethnology and Anthropology of Eurasia. 2011; 39:129–138.10.1016/j.aeae.2011.06.017
18. A high-quality Neandertal genome sequence. <http://www.eva.mpg.de/neandertal/> (
19. Hublin JJ. The origin of Neandertals. Proceedings of the National Academy of Sciences. 2009; 106:16022–16027.10.1073/pnas.0904119106
20. Halestrap AP, Wilson MC. The monocarboxylate transporter family—Role and regulation. IUBMB Life. 2012; 64:109–119.10.1002/iub.572 [PubMed: 22162139]
21. Garcia CK, Goldstein JL, Pathak RK, Anderson RGW, Brown MS. Molecular characterization of a membrane transporter for lactate, pyruvate, and other monocarboxylates: Implications for the Cori cycle. Cell. 1994; 76:865–873. [PubMed: 8124722]
22. Fu S, Watkins Steven M, Hotamisligil Gökhan S. The Role of Endoplasmic Reticulum in Hepatic Lipid Homeostasis and Stress Signaling. Cell metabolism. 2012; 15:623–634. doi:http://dx.doi.org/10.1016/j.cmet.2012.03.007. [PubMed: 22560215]
23. Rhee EP, et al. Lipid profiling identifies a triacylglycerol signature of insulin resistance and improves diabetes prediction in humans. The Journal of clinical investigation. 2011; 121:1402–1411.10.1172/jci44442 [PubMed: 21403394]
24. Savage DB, Semple RK. Recent insights into fatty liver, metabolic dyslipidaemia and their links to insulin resistance. Current Opinion in Lipidology. 2010; 21:329–336. 310.1097/MOL.1090b1013e32833b37782. [PubMed: 20581678]
25. Samuel, Varman T.; Shulman, Gerald I. Mechanisms for Insulin Resistance: Common Threads and Missing Links. Cell. 2012; 148:852–871. [PubMed: 22385956]
26. Florez J, et al. Strong association of socioeconomic status with genetic ancestry in Latinos: implications for admixture studies of type 2 diabetes. Diabetologia. 2009; 52:1528–1536.10.1007/s00125-009-1412-x [PubMed: 19526211]
27. Purcell S, et al. PLINK: A Tool Set for Whole-Genome Association and Population-Based Linkage Analyses. The American Journal of Human Genetics. 2007; 81:559–575.10.1086/519795
28. Alexander DH, Novembre J, Lange K. Fast model-based estimation of ancestry in unrelated individuals. Genome research. 200910.1101/gr.094052.109
29. Risch, N., et al. 12th International Congress of Human Genetics/61st Annual Meeting of The American Society of Human Genetics.;

The SIGMA (Slim Initiative in Genomic Medicine for the Americas) Type 2 Diabetes Genetics Consortium

Writing Team

Amy L. Williams[1,2], Suzanne B. R. Jacobs[1], Hortensia Moreno-Macías[3], Alicia Huerta-Chagoya[4,5], Claire Churchhouse[1], Carla Márquez-Luna[6], Humberto García-Ortíz[6], María José Gómez-Vázquez[4,7], Noël P. Burtt[1], Carlos A. Aguilar-Salinas[4], Clicerio González-Villalpando[8,*], Jose C. Florez[1,9,10,*], Lorena Orozco[6,*], Christopher A. Haiman[11,*], Teresa Tusié-Luna[4,5,*], and David Altshuler[1,2,9,10,12,13,14,*]

[1]Program in Medical and Population Genetics, Broad Institute of Harvard and MIT, Cambridge, Massachusetts, USA
[2]Department of Genetics, Harvard Medical School, Boston, Massachusetts, USA
[3]Universidad Autonoma Metropolitana, Mexico City, Mexico
[4]Instituto Nacional de Ciencias Médicas y Nutrición Salvador Zubirán, Mexico City, Mexico
[5]Instituto de Investigaciones Biomédicas, UNAM. Unidad de Biología Molecular y Medicina Genómica, UNAM/INCMNSZ, Mexico City, Mexico
[6]Instituto Nacional de Medicina Genómica, Mexico City, Mexico
[7]Universidad Autónoma de Nuevo León, San Nicolás de los Garza, Nuevo León 66451, México
[8]Centro de Estudios en Diabetes, Unidad de Investigacion en Diabetes y Riesgo Cardiovascular, Centro de Investigacion en Salud Poblacional, Instituto Nacional de Salud Publica, Mexico City, Mexico
*denotes co-corresponding authors

NIH-PA Author Manuscript

NIH-PA Author Manuscript

NIH-PA Author Manuscript

Analysis Team

Amy L. Williams[1,2], Carla Márquez-Luna[6], Alicia Huerta-Chagoya[4,5], Stephan Ripke[1,15], María José Gómez-Vázquez[4,7], Alisa K. Manning[1], Hortensia Moreno-Macías[3], Humberto García-Ortíz[6], Benjamin Neale[1,15], Noël P. Burtt[1], Carlos A. Aguilar-Salinas[4], David Reich[1,2], Daniel O. Stram[11], Juan Carlos Fernández-López[6], Sandra Romero-Hidalgo[6], David Altshuler[1,2,9,10,12,13,14], Jose C. Florez[1,8,10], Teresa Tusié-Luna[4,5], Nick Patterson[1], and Christopher A. Haiman[11]

Clinical Research, Study Design and Metabolic Phenotyping

Diabetes in Mexico Study: Irma Aguilar-Delfín[6], Angélica Martínez-Hernández[6], Federico Centeno-Cruz[6], Elvia Mendoza-Caamal[6], Cristina Revilla-Monsalve[16], Sergio Islas-Andrade[16], Emilio Córdova[6], Eunice Rodríguez-Arellano[17], Xavier Soberón[6], and Lorena Orozco[6]

Massachusetts General Hospital: Jose C. Florez[1,9,10]

Mexico City Diabetes Study: Clicerio González-Villalpando[8] and María Elena González-Villalpando[8]

Multiethnic Cohort Study: Christopher A. Haiman[11], Brian E. Henderson[11], Kristine Monroe[11], Lynne Wilkens[18], Laurence N. Kolonel[18], and Loic Le Marchand[18]

UNAM/INCMNSZ Diabetes Study: Laura Riba[5], María Luisa Ordóñez-Sánchez[4], Rosario Rodríguez-Guillén[4], Ivette Cruz-Bautista[4], Maribel Rodríguez-Torres[4], Linda Liliana Muñoz-Hernández[4], Tamara Sáenz[4], Donají Gómez[4], and Ulices Alvirde[4]

Sample QC and Whole Genome Genotyping

Noël P. Burtt[1], Robert C. Onofrio[19], Wendy M. Brodeur[19], Diane Gage[19], Jacquelyn Murphy[1], Jennifer Franklin[19], Scott Mahan[19], Kristin Ardlie[19], Andrew T. Crenshaw[19], and Wendy Winckler[19]

[9]Center for Human Genetic Research and Diabetes Research Center (Diabetes Unit), Massachusetts General Hospital, Boston, Massachusetts, USA
[10]Department of Medicine, Harvard Medical School, Boston, Massachusetts, USA
[11]Department of Preventive Medicine, Keck School of Medicine, University of Southern California, Los Angeles, California,, USA
[12]Center for Human Genetic Research, Massachusetts General Hospital, Boston, Massachusetts, USA
[13]Department of Molecular Biology, Harvard Medical School, Boston, Massachusetts, USA
[14]Department of Biology, Massachusetts Institute of Technology, Cambridge, Massachusetts, USA
[15]Analytic and Translational Genetics Unit, Massachusetts General Hospital, Boston, MA, USA
[16]Instituto Mexicano del Seguro Social SXXI, Mexico City, Mexico
[17]Instituto de Seguridad y Servicios Sociales para los Trabajadores del Estado, Mexico City, Mexico
[18]Epidemiology Program, University of Hawaii Cancer Center, Honolulu, Hawaii, USA
[19]The Genomics Platform, The Broad Institute of Harvard and MIT, Cambridge, Massachusetts, USA

NIH-PA Author Manuscript

NIH-PA Author Manuscript

NIH-PA Author Manuscript

Neandertal analysis team

Kay Prüfer[20], Michael V. Shunkov[21], Susanna Sawyer[20], Udo Stenzel[20], Janet Kelso[20], Monkol Lek[1,15], Sriram Sankararaman[1,2], Amy L. Williams[1,2], Nick Patterson[1], Daniel G. MacArthur[1,15], David Reich[1,2], Anatoli P. Derevianko[21], and Svante Pääbo[20]

Functional analysis and metabolite profiling

Suzanne B. R. Jacobs[1], Claire Churchhouse[1], Shuba Gopal[22], James A. Grammatikos[22], Ian C. Smith[23], Kevin H. Bullock[22], Amy A. Deik[22], Amanda L. Souza[22], Kerry A. Pierce[22], Clary B. Clish[22], and David Altshuler[1,2,9,10,12,13,14]

Replication genotyping and analysis

Broad Institute of Harvard and MIT: Timothy Fennell[19], Yossi Farjoun[19], Broad Genomics Platform[19], and Stacey Gabriel[19]

Singapore Chinese Health Study: Daniel O. Stram[11], Myron D. Gross[24], Mark A. Pereira[24], Mark Seielstad[25], Woon-Puay Koh[26,27], and E-Shyong Tai[26,27,28]

T2D-GENES Consortium: Jason Flannick[1,9], Pierre Fontanillas[1], Andrew Morris[29], Tanya M. Teslovich[30], Noël P. Burtt[1], Gil Atzmon[31], John Blangero[32], Don W. Bowden[33], John Chambers[34,35,36], Yoon Shin Cho[37], Ravindranath Duggirala[32], Benjamin Glaser[38,39], Craig Hanis[40], Jaspal Kooner[35,36,41], Markku Laakso[42], Jong-Young Lee[43],

[20]Department of Evolutionary Genetics, Max Planck Institute for Evolutionary Anthropology, D-04103 Leipzig, Germany
[21]Palaeolithic Department, Institute of Archaeology and Ethnography, Russian Academy of Sciences, Siberian Branch, 630090 Novosibirsk, Russia
[22]The Metabolite Profiling Platform, The Broad Institute of Harvard and MIT, Cambridge, Massachusetts, USA
[23]Cancer Biology Program, The Broad Institute of Harvard and MIT, Cambridge, Massachusetts, USA
[24]University of Minnesota, Minneapolis, Minnesota, USA
[25]University of California San Francisco, San Francisco, California, USA
[26]Duke-National University of Singapore Graduate Medical School, Singapore, Singapore
[27]Saw Swee Hock School of Public Health, National University of Singapore, Singapore
[29]Wellcome Trust Centre for Human Genetics, University of Oxford, Oxford, UK
[30]Department of Biostatistics, Center for Statistical Genetics, University of Michigan, Ann Arbor, Michigan, USA
[31]Department of Medicine, Department of Genetics, Albert Einstein College of Medicine, Bronx, New York, USA
[32]Department of Genetics, Texas Biomedical Research Institute, San Antonio, Texas, USA
[33]Center for Genomics and Personalized Medicine Research, Center for Diabetes Research, Department of Biochemistry, Department of Internal Medicine, Wake Forest School of Medicine, Winston-Salem, North Carolina, USA
[34]Department of Epidemiology and Biostatistics, Imperial College London, London, UK
[35]Imperial College Healthcare NHS Trust, London, UK.
[36]Ealing Hospital National Health Service (NHS) Trust, Middlesex, UK
[37]Department of Biomedical Science, Hallym University, Chuncheon, Gangwon-do, Korea
[38]Endocrinology and Metabolism Service, Hadassah-Hebrew University Medical School, Jerusalem, Israel
[39]Israel Diabetes Research Group (IDRG), Israel
[40]Human Genetics Center, University of Texas Health Science Center at Houston, Houston, Texas, USA
[41]National Heart and Lung Institute (NHLI), Imperial College London, Hammersmith Hospital, London, UK
[42]Department of Medicine, University of Eastern Finland, Kuopio Campus and Kuopio University Hospital, Kuopio, Finland
[43]Center for Genome Science, National Institute of Health, Osong Health Technology Administration Complex, Chungcheongbuk-do, Cheongwon-gun, Gangoe-myeon, Yeonje-ri, Korea

NIH-PA Author Manuscript

NIH-PA Author Manuscript

NIH-PA Author Manuscript

E-Shyong Tai[26,27,28], Yik Ying Teo[44,45,46,47,48], James G. Wilson[49], and the T2D-GENES Consortium

Multiethnic Cohort Study: Christopher A. Haiman[11], Brian E. Henderson[11], Kristine Monroe[11], Lynne Wilkens[18], Laurence N. Kolonel[18], and Loic Le Marchand[18]

Texas Biomedical Research Institute and University of Texas Health Science Center at San Antonio: Sobha Puppala[32], Vidya S. Farook[32], Farook Thameem[50], Hanna E. Abboud[50], Ralph A. DeFronzo[51], Christopher P. Jenkinson[51], Donna M. Lehman[52], Joanne E. Curran[32], John Blangero[32], and Ravindranath Duggirala[32]

Scientific and Project Management

Noël P. Burtt[1] and Maria L. Cortes[53]

Steering Committee

David Altshuler[1,2,9,10,12,13,14], Jose C. Florez[1,9,10], Christopher A. Haiman[11], Brian E. Henderson[11], Carlos A. Aguilar-Salinas[4], Clicerio González-Villalpando[8], Lorena Orozco[6], and Teresa Tusié-Luna[4,5]

[28]Department of Medicine, Yong Loo Lin School of Medicine, National University of Singapore, Singapore
[44]Department of Epidemiology and Public Health, National University of Singapore, Singapore, Singapore
[45]Centre for Molecular Epidemiology, National University of Singapore, Singapore, Singapore
[46]Genome Institute of Singapore, Agency for Science, Technology and Research, Singapore, Singapore
[47]Graduate School for Integrative Science and Engineering, National University of Singapore, Singapore, Singapore
[48]Department of Statistics and Applied Probability, National University of Singapore, Singapore, Singapore.
[49]Department of Physiology and Biophysics, University of Mississippi Medical Center, Jackson, Mississippi, USA
[50]Division of Nephrology, Department of Medicine, University of Texas Health Science Center at San Antonio, San Antonio, Texas
[51]Division of Diabetes, Department of Medicine, University of Texas Health Science Center at San Antonio, San Antonio, Texas
[52]Division of Clinical Epidemiology, Department of Medicine, University of Texas Health Science Center at San Antonio, San Antonio, Texas
[53]Broad Institute of Harvard and MIT, Cambridge, Massachusetts, USA

NIH-PA Author Manuscript

NIH-PA Author Manuscript

NIH-PA Author Manuscript

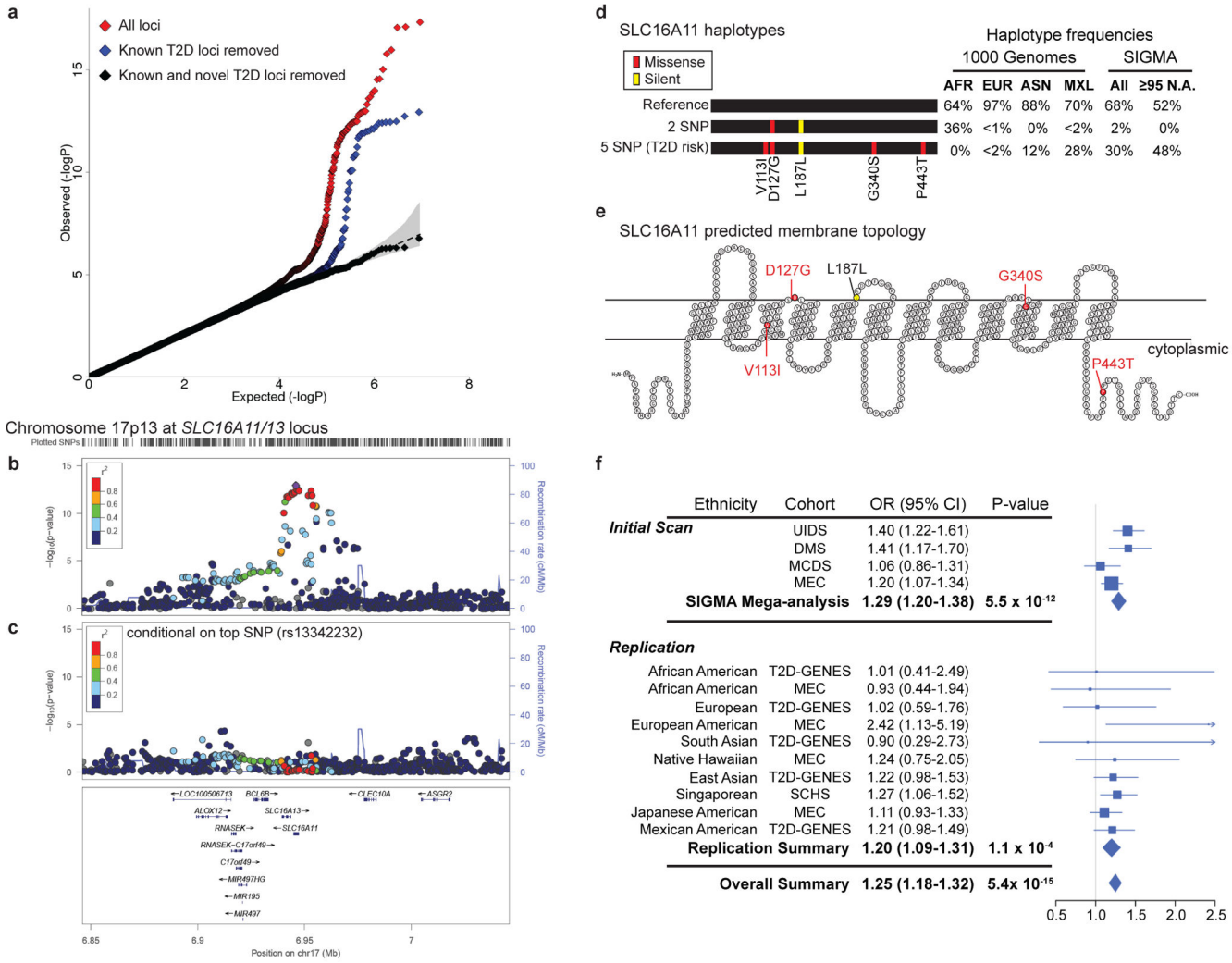

Figure 1. Identification of a novel T2D risk haplotype carrying 5 SNPs in SLC16A11

(a) QQ plot of association statistics in genome-wide scan shows calibration under the null and enrichment in the tail for all SNPs (*red*), and after removing SNPs within 1 Mb of previously published T2D associations (*blue*). Removal of sites within 1 Mb of 68 known loci and two novel loci results in a null distribution (*black*). **(b)** Regional plot of association at 17p13.1 that spans *SLC16A11* and *SLC16A13*. **(c)** Analysis conditional on genotype at rs13342232 (the top associated variant) reduces signal to far below genome-wide significance across the surrounding region. Color indicates r^2 to the most strongly associated site; recombination rate is shown, each based on the 1,000 Genomes ASN population. (**d**) Graphical depictions of SLC16A11 haplotypes constructed from the synonymous and four missense SNPs associated to T2D, with haplotype frequencies derived from the 1,000 Genomes Project and SIGMA samples. AFR, Africa (*n*=185); EUR, European (*n*=379); ASN, East Asian (*n*=286); MXL, Mexican samples from Los Angeles (*n*=66). Frequencies from SIGMA samples are calculated from genotypes and represent either the entire dataset ("All") or only samples estimated to have ≥95% Native American ancestry ("≥95 N.A.", *n*=290; Supplementary Note). Haplotypes with population frequency <1% are not depicted.

(**e**) Predicted membrane topology of human SLC16A11 generated using TMHMM 2.0 and visualized with TeXtopo. Locations of SNPs carried by the T2D-associated haplotype are indicated. (**f**) Forest plot depicting odds ratio estimates at rs75493593 from the four SIGMA cohorts, the SIGMA pooled mega-analysis, the replication cohorts, replication-only meta-analysis, and the overall meta-analysis (including all replication cohorts and the SIGMA mega-analysis). Accompanying table lists ethnicity, cohort names, estimated odds ratio (OR) and 95% confidence interval (95% CI). Replication cohorts are the Type 2 Diabetes Genetic Exploration by Next-generation sequencing in multi-Ethnic Samples (T2D-GENES), Multiethnic Cohort (MEC), and Singapore Chinese Health Study (SCHS). Further details provided in Supplementary Table 8.

NIH-PA Author Manuscript
NIH-PA Author Manuscript
NIH-PA Author Manuscript

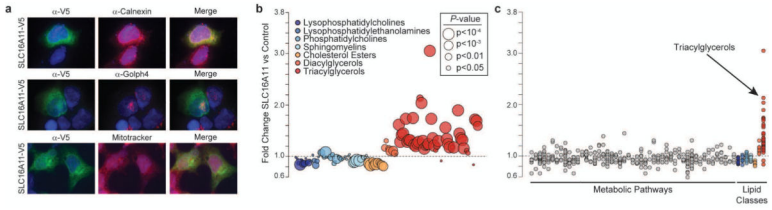

Figure 2. SLC16A11 localizes to the endoplasmic reticulum and alters lipid metabolism in HeLa cells

(a) Localization of SLC16A11 to the endoplasmic reticulum. HeLa cells expressing C-terminus, V5-tagged SLC16A11 were immunostained for SLC16 expression (α-V5) along with markers for the endoplasmic reticulum (α-Calnexin), cis-Golgi apparatus (α-Golph4), or mitochondria (MitoTracker). Imaging of each protein was optimized for clarity of localization rather than comparison of expression level across proteins. **(b)** Changes in intracellular lipid metabolites following expression of SLC16A11-V5 in HeLa cells. The fold-change in cells expressing SLC16A11 relative to cells expressing control proteins is plotted for individual lipid metabolites, with lipid classes indicated by point color and *P*-values (of the Wilcox rank sum test) by point size. **(c)** Fold change plotted for both polar and lipid metabolites, grouped according to metabolic pathway or class. Each point within a pathway or class shows the fold-change of a single metabolite within that pathway or class. Pathway names and statistical analyses are shown in Extended Data Fig. 10 and Supplementary Table 14.

NIH-PA Author Manuscript
NIH-PA Author Manuscript
NIH-PA Author Manuscript

NIH-PA Author Manuscript
NIH-PA Author Manuscript
NIH-PA Author Manuscript

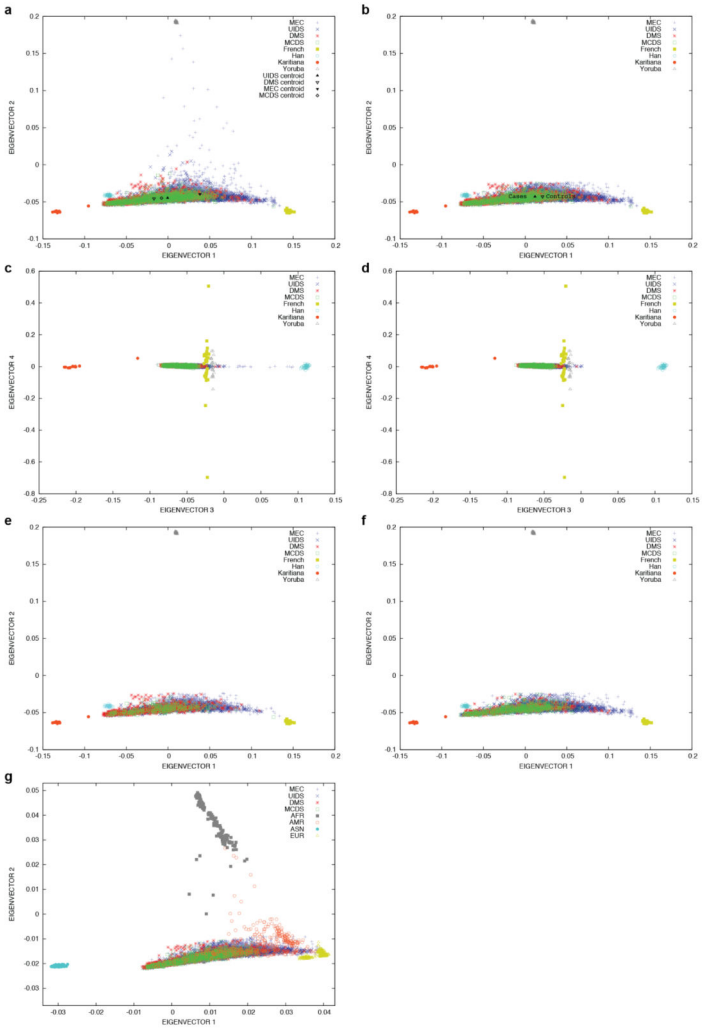

Extended Data Figure 1. Principle component analysis (PCA) projection of SIGMA samples onto principal components calculated using data from samples collected by the Human Genome Diversity Project (HGDP)

PCA projection of SIGMA onto HGDP Yoruba, French, Karitiana and Han (Chinese) populations **(a)** before ancestry quality control filters were applied, with cohort centroids as indicated and **(b)** after all quality control filters were applied, with case and control centroids as indicated. Principal components 3 and 4 **(c)** before filtering samples on ancestry (a small number of samples in the MEC cohort show East Asian admixture) and **(d)** after all quality control filters were applied. Additional plots as in (b) but separating **(e)** cases and **(f)** controls.

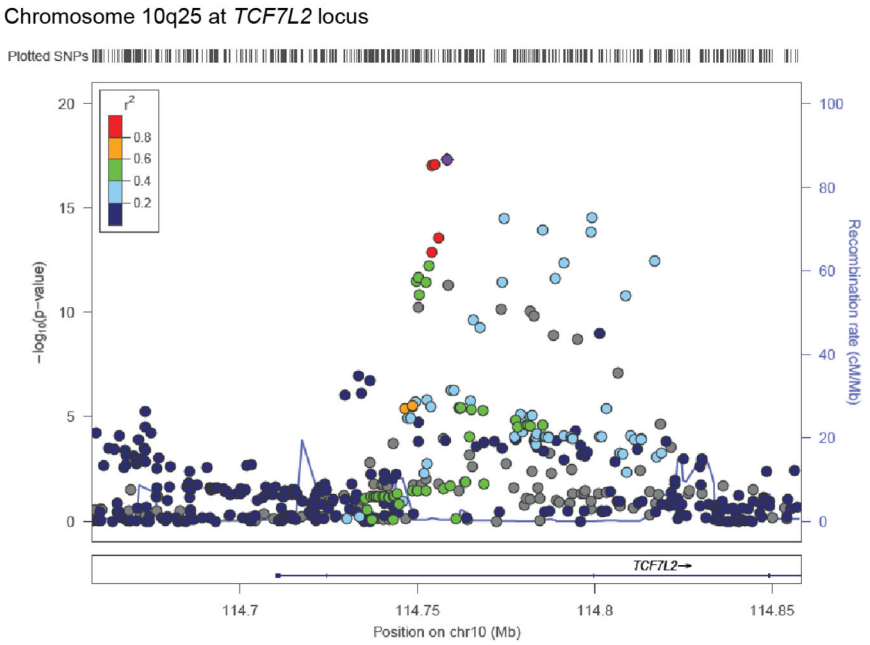

Extended Data Figure 2. Regional plot for signal at *TCF7L2*

Point color indicates r^2 to the most strongly associated site (rs7903146) and recombination rate is also shown, both based on the 1,000 Genomes ASN population.

NIH-PA Author Manuscript
NIH-PA Author Manuscript
NIH-PA Author Manuscript

NIH-PA Author Manuscript
NIH-PA Author Manuscript
NIH-PA Author Manuscript

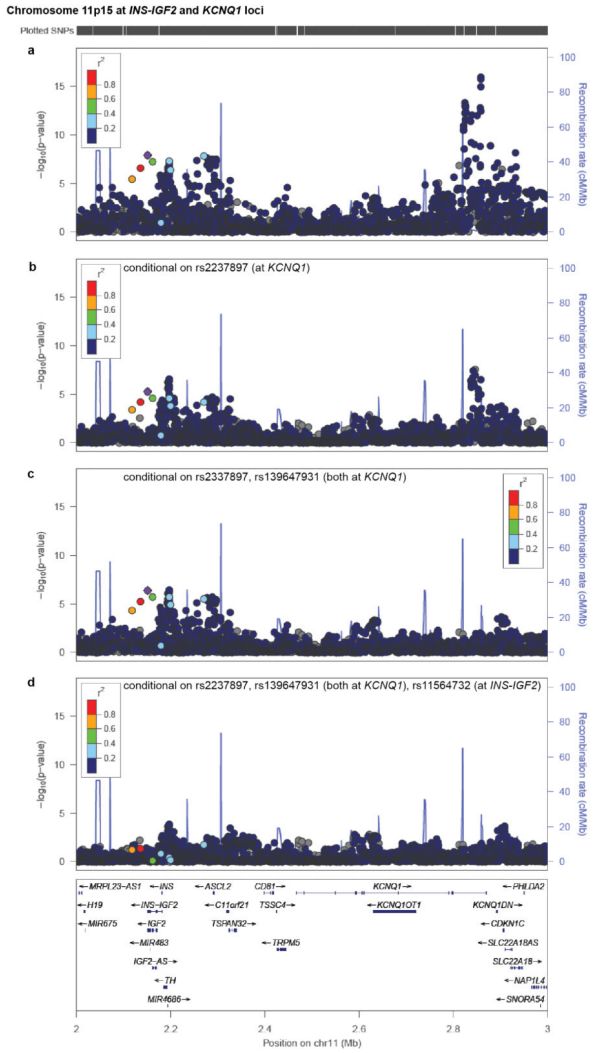

Extended Data Figure 3. Conditional analyses reveal multiple independent signals at *INS-IGF2* and *KCNQ1*

Regional plots are shown for the interval spanning *INS-IGF2* and *KCNQ1* **(a)** without conditioning, **(b)** conditional on rs2237897 at *KCNQ1*, **(c)** conditional on rs2237897 and rs139647931 (both at *KCNQ1*), and **(d)** conditional on rs2237897 and rs139647931 (both at *KCNQ1*) and rs11564732 (the top associated variant in the *INS-IGF2-TH* region). The top SNPs in 11p15.5 and *KCNQ1* are ~700 kb away from each other, but despite this proximity, there is a strong residual signal of association at *INS-IGF2* after analysis conditional on genotype at *KCNQ1*. Point color indicates r^2 to rs11564732 and recombination rate is also shown, both based on the 1,000 Genomes ASN population.

NIH-PA Author Manuscript
NIH-PA Author Manuscript
NIH-PA Author Manuscript

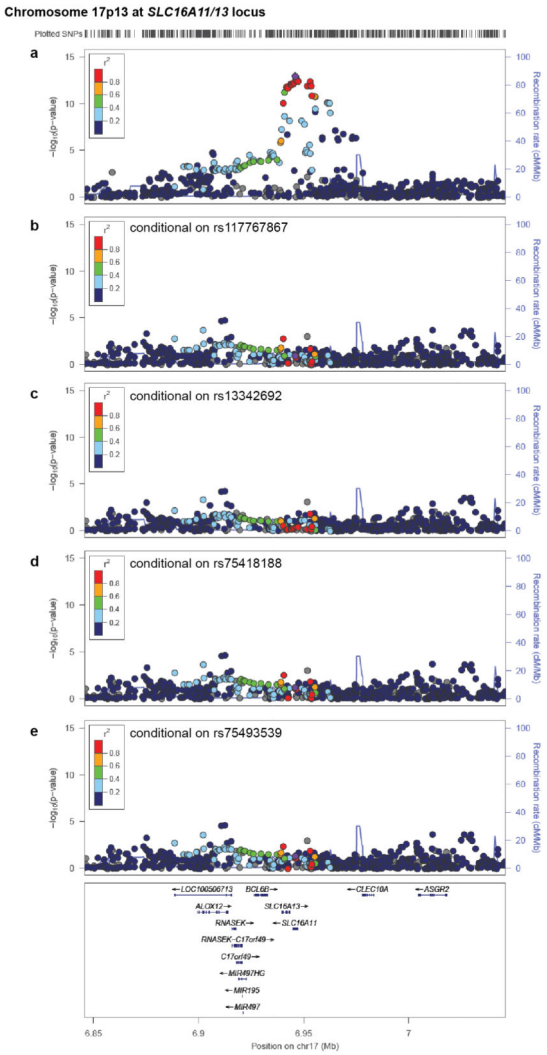

Extended Data Figure 4. Regional plots for *SLC16A11* conditional on associated missense variants of that gene

Association signal at chromosome 17p13 (**a**) without conditioning, or conditional on the four missense SNPs in SLC16A11: **(b)** rs117767867, **(c)** rs13342692, **(d)** rs75418188, and **(e)** rs75493593. Point color indicates r^2 to the most strongly associated SNP (rs13342232) and recombination rate is also shown, both based on the 1,000 Genomes ASN population.

NIH-PA Author Manuscript
NIH-PA Author Manuscript
NIH-PA Author Manuscript

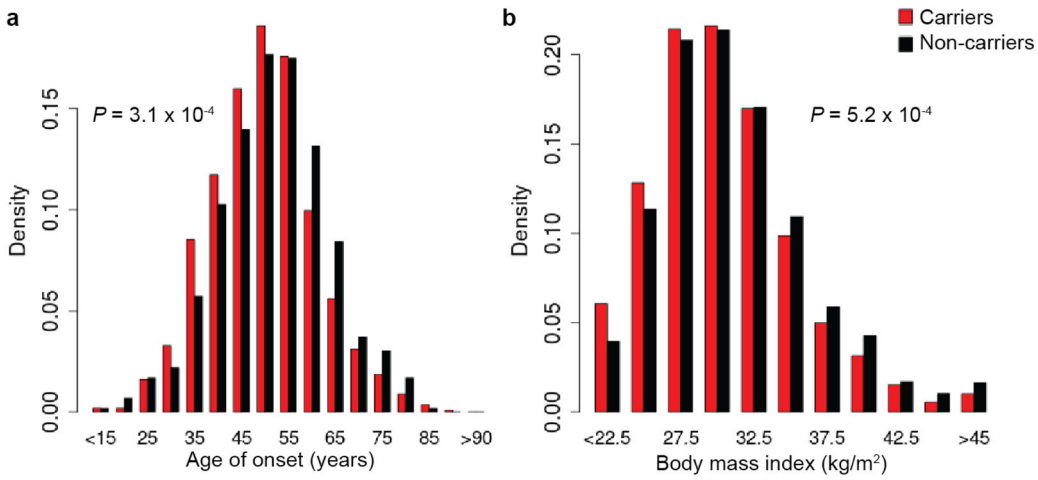

Extended Data Figure 5. Cases with risk haplotype develop T2D younger and at a lower BMI than non-carriers

(**a**) Distribution of age-of-onset in T2D cases based on genotype at rs13342232, binned every 5 years with upper bounds indicated (carriers *n*=1,126; non-carriers *n*=594). (**b**) Distribution of BMI in T2D cases for carriers and non-carriers of rs13342232, binned every 2.5 kg/m^2 with upper bounds indicated (carriers *n*=2,161; non-carriers *n*=1,647). P-values from two-sample t-test between T2D risk haplotype carriers and T2D non-carriers.

NIH-PA Author Manuscript
NIH-PA Author Manuscript
NIH-PA Author Manuscript

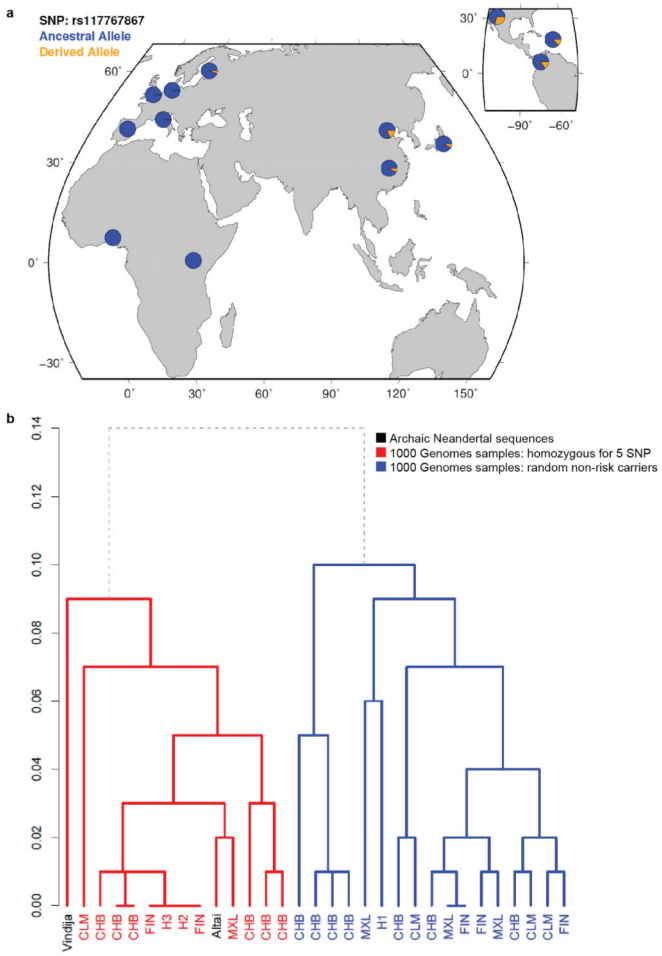

Extended Data Figure 6. Frequency distribution of the risk haplotype and dendrogram depicting clustering with Neandertal haplotypes

(a) Allele frequency of missense SNP rs117767867 (tag for risk haplotype) in the 1,000 Genomes Phase I dataset**. (b)** Dendrogram generated from haplotypes across the 73 kb Neandertal introgressed region. Nodes for modern human haplotypes are labeled in red or blue with the 1,000 Genomes population in which the corresponding haplotype resides. Archaic Neandertal sequences are labeled in black and include the low coverage Neandertal sequence[15] (labeled Vindija), and the unpublished Neandertal sequence that is homozygous for the 5 SNP risk haplotype[18] (Altai). H1 includes haplotypes from MXL and FIN, and H2 and H3 both include haplotypes from CLM, MXL, CHB, and ASW. Modern human sequences included are all 1,000 Genomes Phase I samples that are homozygous for the 5 SNP risk haplotype (*n*=15), and 16 non-risk haplotypes—four haplotypes (from two randomly selected individuals) from each of the CLM, MXL, CHB, and FIN 1,000 Genomes populations (the populations with carriers of the 5 SNP haplotype). The red subtree depicts the Neandertal clade, with all risk haplotypes clustering with the Altai and Vindija sequences. In blue are all other modern human haplotypes. The dendrogram was generated by the R function *hclust* using a complete linkage clustering algorithm on a distance matrix measuring the fraction of SNPs called in the 1000 genomes project at which a pair of

haplotypes differs (the Y-axis represents this distance). Since haplotypes are unavailable for the archaic samples, we picked a random allele to compute the distance matrix.

NIH-PA Author Manuscript
NIH-PA Author Manuscript
NIH-PA Author Manuscript

NIH-PA Author Manuscript
NIH-PA Author Manuscript
NIH-PA Author Manuscript

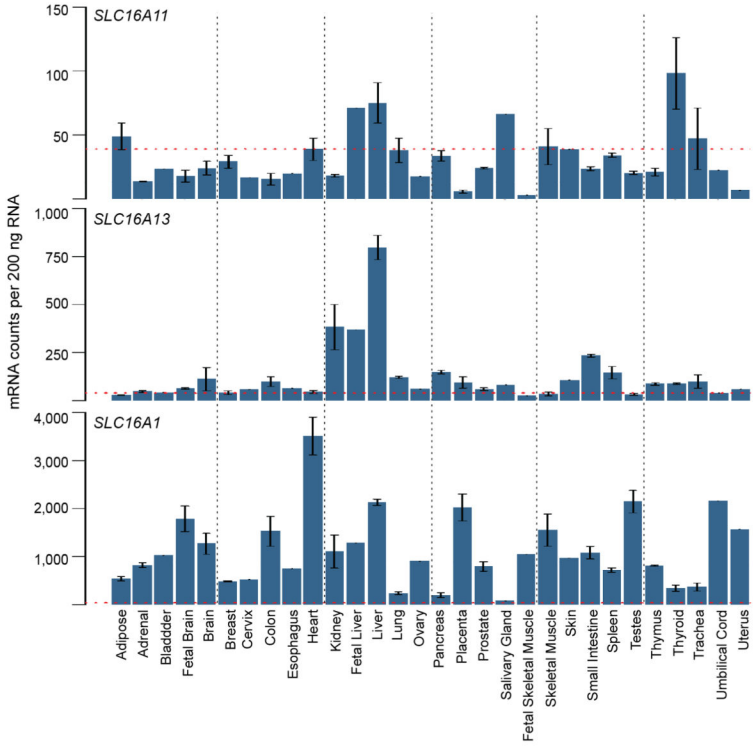

Extended Data Figure 7. Analysis of gene expression for *SLC16A11*, *SLC16A13*, and *SLC16A1* in 30 human tissues

Data measured using nCounter is shown as mean, normalized mRNA counts per 200ng RNA +/− SEM. Threshold for background (non-specific) binding is indicated by the red line. Sample size for each tissue (*n*): pancreas (5), adipose, brain, colon, liver, skeletal muscle, and thyroid (3), adrenal, fetal brain, breast, heart, kidney, lung, placenta, prostate, small intestine, spleen, testes, thymus, and trachea (2), bladder, cervix, esophagus, fetal liver, ovary, salivary gland, fetal skeletal muscle, skin, umbilical cord, and uterus (1).

NIH-PA Author Manuscript

NIH-PA Author Manuscript

NIH-PA Author Manuscript

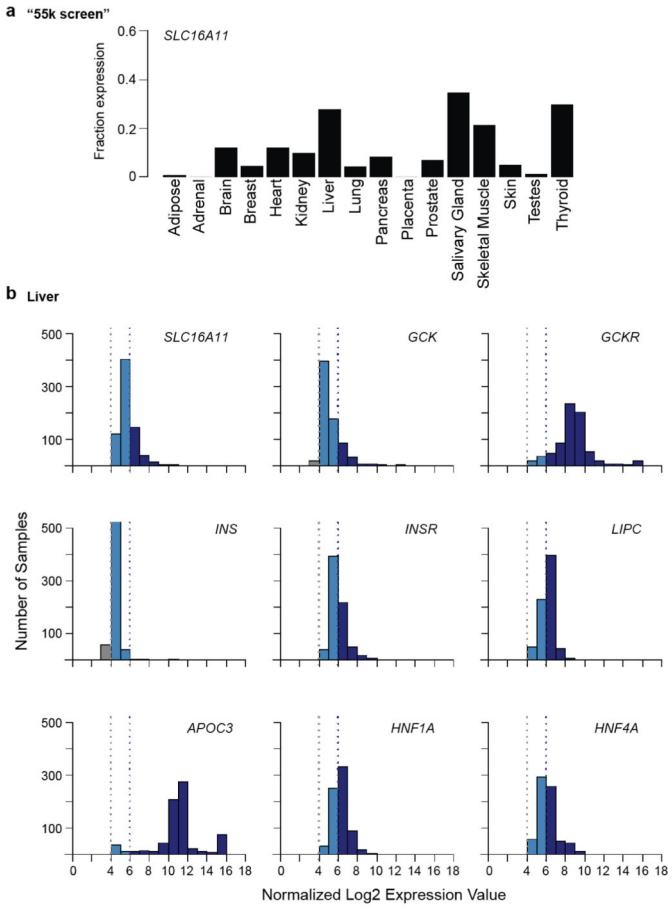

Extended Data Figure 8. Microarray-based analysis of *SLC16A11* expression in human tissues

(**a**) Results from the "55k screen", a survey of gene expression in 55,269 samples profiled on the Affymetrix U133 plus 2.0 array, are shown as the fraction of samples of a given tissue in which *SLC16A11* is expressed. Sample size for each tissue (*n*): adipose (394), adrenal (69), brain (1990), breast (4104), heart (178), kidney (675), liver (721), lung (1442), pancreas (150), placenta (107), prostate (578), salivary gland (26), skeletal muscle (793), skin (947), testis (102), thyroid (108). (**b**) Histograms show the expression level distribution *of SLC16A11* and other well-studied liver genes in 721 liver samples from the "55k screen." *INS* is shown as reference for a gene not expressed in liver. Based on negative controls a normalized log2 expression of 4 is considered baseline and log2 expression values greater than 6 are considered expressed.

NIH-PA Author Manuscript
NIH-PA Author Manuscript
NIH-PA Author Manuscript

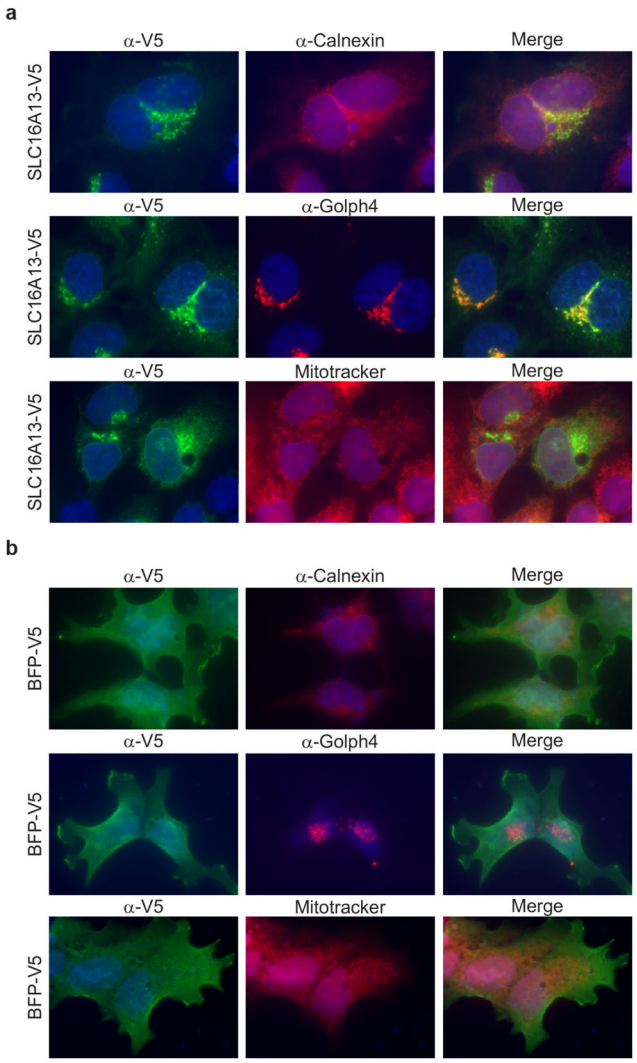

Extended Data Figure 9. SLC16A13 localizes to Golgi apparatus

HeLa cells transiently expressing C-terminus, V5-tagged (**a**) SLC16A13 or (**b**) BFP were immunostained for SLC16A13 or BFP expression (α-V5) along with specific markers for the endoplasmic reticulum (α-Calnexin), cis-Golgi apparatus (α-Golph4) and mitochondria (MitoTracker). Due to heterogeneity in expression levels of overexpressed proteins and endogenous organelle markers, imaging of each protein was optimized for clarity of localization and varied across images; therefore, images are not representative of relative expression levels of each protein as compared to the other proteins.

NIH-PA Author Manuscript
NIH-PA Author Manuscript
NIH-PA Author Manuscript

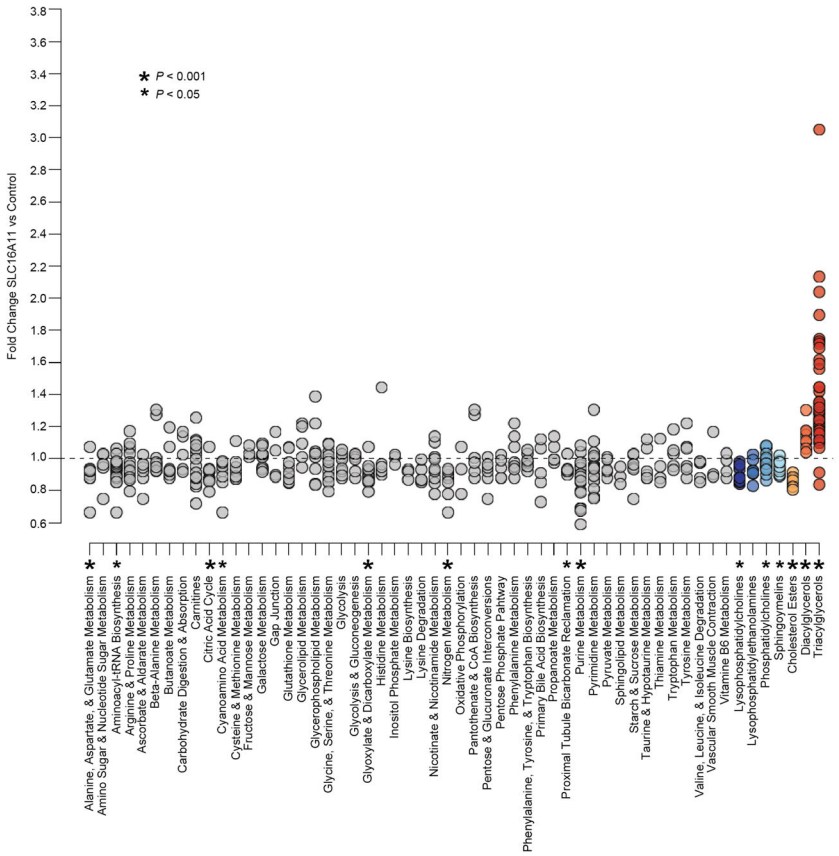

Extended Data Figure 10. Pathway and class-based metabolic changes induced by SLC16A11 expression

Changes in metabolite levels in HeLa cells expressing SLC16A11-V5 compared to control-transfected cells are plotted in groups according to metabolic pathway or class. Pathways shown include all KEGG pathways from the human reference set for which metabolites were measured as well as eight additional classes of metabolites covering carnitines and lipid sub-types. Each point within a pathway or class shows the fold-change of a single metabolite within that pathway or class. For each pathway or class with at least six measured metabolites, enrichment was computed as described in Online Methods. *Asterisks* indicate pathways with $P \leq 0.05$ and $FDR \leq 0.25$. Supplementary Table 14 shows additional details from the enrichment analysis.

NIH-PA Author Manuscript NIH-PA Author Manuscript NIH-PA Author Manuscript

Nature. Author manuscript; available in PMC 2014 August 09.

Table 1

Study cohorts comprising the SIGMA T2D Project dataset with sample location, study design, numbers of cases and controls (including numbers before quality control (QC) checks), % male participants, age ± standard deviation (SD), age-of-onset in cases ± SD, body mass index ± SD, and fasting plasma glucose in controls ± SD.

Study	Sample Location	Study Design		N (Before QC)	% Male	Age (years)	Age-of- onset (years)	Body mass index (kg/m^2)	Fasting plasma glucose (mmol/l)
UNAM/INCMNSZ Diabetes Study (UIDS)	Mexico City, Mexico	Prospective Cohort	Controls	1,138 (1,195)	41.1%	55.3 ± 9.4	–	28.1 ± 4.0	4.8 ± 0.5
			T2D Cases	815 (872)	40.9%	56.2 ± 12.3	44.2 ± 11.3	28.4 ± 4.5	–
Diabetes in Mexico Study (DMS)	Mexico City, Mexico	Prospective Cohort	Controls	472 (505)	25.8%	52.5 ± 7.7	–	28.0 ± 4.4	5.0 ± 0.4
			T2D Cases	690 (762)	33.0%	55.8 ± 11.1	47.8 ± 10.6	29.0 ± 5.4	–
Mexico City Diabetes Study (MCDS)	Mexico City, Mexico	Prospective Cohort	Controls	613 (790)	39.3%	62.5 ± 7.7	–	29.4 ± 4.8	5.0 ± 0.5
			T2D Cases	287 (358)	41.1%	64.2 ± 7.5	55.1 ± 9.7	29.9 ± 5.4	–
Multiethnic Cohort (MEC)	Los Angeles, California, USA	Case- Control	Controls	2,143 (2,464)	48.3%	59.3 ± 7.0	–	26.6 ± 3.9	N/A
			T2D Cases	2,056 (2,279)	47.9%	59.2 ± 6.9	N/A	30.0 ± 5.4	–